Available online at www.sciencedirect.com
SCIENCE DIRECT
ELSEVIER
International Journal of Machine Tools & Manufacture 46 (2006) 518–530
INTERNATIONAL JOURNAL OF MACHINE TOOLS & MANUFACTURE DESIGN, RESEARCH AND APPLICATION
www.elsevier.com/locate/ijmactool

The influence of friction models on finite element simulations of machining

Tugrul Özel*

Department of Industrial and Systems Engineering, Rutgers, The State University of New Jersey, Piscataway, New Jersey 08854 USA

Received 30 April 2004; accepted 4 July 2005
Available online 19 August 2005

Abstract

In the analysis of orthogonal cutting process using finite element (FE) simulations, predictions are greatly influenced by two major factors; a) flow stress characteristics of work material at cutting regimes and b) friction characteristics mainly at the tool-chip interface. The uncertainty of work material flow stress upon FE simulations may be low when there is a constitutive model for work material that is obtained empirically from high-strain rate and temperature deformation tests. However, the difficulty arises when one needs to implement accurate friction models for cutting simulations using a particular FE formulation. In this study, an updated Lagrangian finite element formulation is used to simulate continuous chip formation process in orthogonal cutting of low carbon free-cutting steel. Experimentally measured stress distributions on the tool rake face are utilized in developing several different friction models. The effects of tool-chip interfacial friction models on the FE simulations are investigated. The comparison results depict that the friction modeling at the tool-chip interface has significant influence on the FE simulations of machining. Specifically, variable friction models that are developed from the experimentally measured normal and frictional stresses at the tool rake face resulted in most favorable predictions. Predictions presented in this work also justify that the FE simulation technique used for orthogonal cutting process can be an accurate and viable analysis as long as flow stress behavior of the work material is valid at the machining regimes and the friction characteristics at the tool-chip interface is modeled properly.

1. Introduction

There has been considerable amount of research devoted to develop analytical, mechanistic and Finite Element Method (FEM) based numerical models to simulate metal cutting processes. Among those, FEM based simulation models are highly essential in predicting chip formation, computing distributions of strain, strain rate, temperatures and stresses on the cutting edge, in the chip and on the machined work surface [1,2]. The premise of FEM based simulation models is their potential upon leading further predictions in wear and fracture of the cutting tool and integrity (residual stresses, microhardness and microstructure) of machined surfaces.

In metal cutting, severe deformations take place in the shearing zones and in the vicinity of the cutting edge where high strain-rates and temperatures are observed. There are two main shearing zones due to shearing and friction as shown in Fig. 1. The primary shear zone is where the major shearing of work material takes place. Also a secondary shear zone exists adjacent to the tool-chip interface due to high stress contact conditions. Work material deformation behavior in primary and secondary zones is highly sensitive to the cutting conditions. The frictional conditions between the tool and the workpiece as well as at the tool-chip interface are highly complex and they are at least as important as flow stress characterization of the work material. As a result, the stresses and temperatures at the tool-chip interface and around the cutting edge can be very high in some cutting conditions, causing excessive tool wear and tool 'chipping' fracture. Therefore, accurate predictions for the distributions of the process variables such as stresses and temperatures with Finite Element (FE) simulations are imperative to identify optimum cutting conditions, tool material, edge geometry and coating in order to help improve the quality of machined surfaces and the overall productivity.

However, the effects of work material flow stress constitutive models and the influence of the tool-chip

* Corresponding author. Tel.: +1 732 445 1099; fax: +1 732 445 5467.
E-mail address: ozel@rci.rutgers.edu.

0890-6955/$ - see front matter © 2005 Elsevier Ltd. All rights reserved.
doi:10.1016/j.ijmachtools.2005.07.001

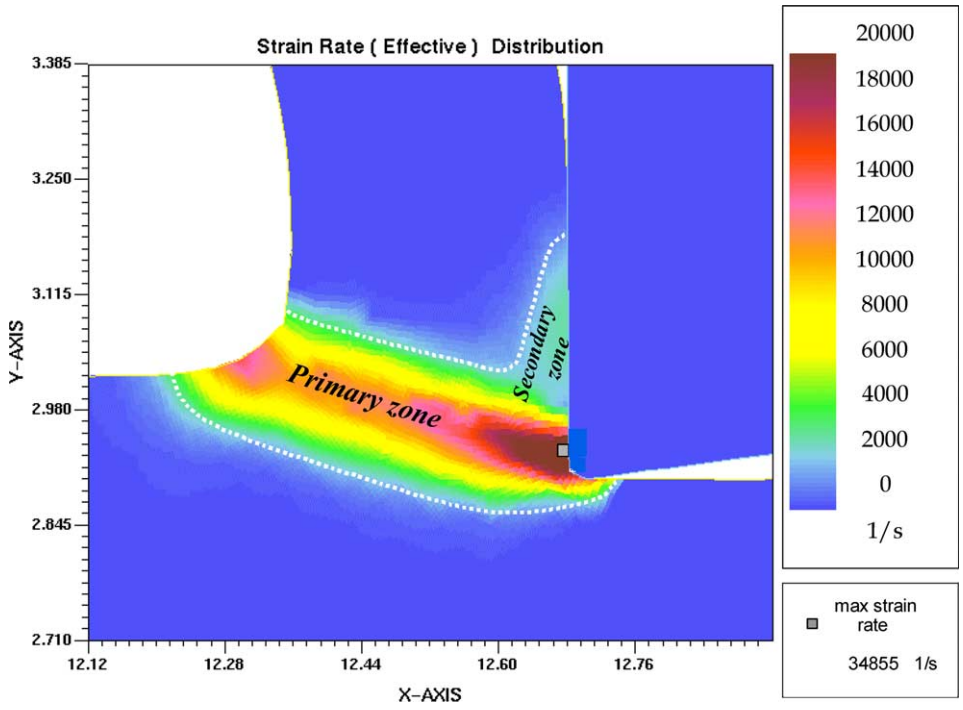

Fig. 1. Deformation zones in orthogonal cutting as obtained from FE simulations.

interfacial friction models on the accuracy of the predicted process variables in FE simulations have not been adequately understood. Specifically, application of realistic friction models that are based on process variables such as stresses and temperatures should to be and their influence on predicted process variables should to be assessed.

In all of the analysis of orthogonal cutting process using FE simulations, predictions are greatly influenced by two major factors; a) flow stress characteristics of work material at cutting regimes and b) friction characteristics at the tool-chip interface. The uncertainty of work material flow stress upon FE simulations may be low when there is a constitutive model for work material that is obtained empirically from high-strain rate and temperature deformation tests. However, the difficulty arises when one needs to implement accurate friction and contact conditions for cutting simulations using a particular FE formulation. This is not to undermine the importance of flow stress characterization for metal cutting regimes but to rather investigate the friction characterization at the tool-chip interface, which remains as an important issue to be researched for the success of the FE simulations of machining. Consequently, the objective of this study is to address the friction-modeling problem and its influence upon the FE simulations of orthogonal cutting.

2. Literature review

A review of the technical literature reveals that currently FE modeling of cutting is not fully capable of simulating practical machining operations [1,2]. In other words, the complexity and the diversity of cutting processes are such that a single process model or simulation cannot be applied to all materials and cutting conditions.

In continuum-based FEM modeling of cutting, there are two types of analysis in which a continuous medium can be described: Eulerian and Lagrangian. In a Lagrangian analysis, the computational grid deforms with the material whereas in a Eulerian analysis it is fixed in space. The Lagrangian calculation embeds a computational mesh in the material domain and solves for the position of the mesh at discrete points in time. In implementing those analyses, two distinct methods, the implicit and explicit time integration techniques, can be utilized.

Some researchers used the Eulerian formulation to model orthogonal metal cutting as continuous chip formation at steady state [3,4,5,6,7,8]. The advantage of using Eulerian formulation is that fewer elements required in modeling the workpiece and the chip, thereby reducing the computation time. The drawback of such an approach was a need in determining chip geometry and shear angle experimentally prior to the simulation. However, a vast majority of models was based on the Lagrangian formulation, which allows the chip to be modeled from incipient to steady state [9,10,11,12,13,14,15,16,17,18,19].

Using the Lagrangian formulation with no adequate remeshing requires a criterion for separation of the chip from the workpiece. As a result, the development of a realistic separation criterion has been an important factor in earlier FE modeling of cutting with Lagrangian formulation approaches. Black and Huang [20] carried a rigorous evaluation for the chip separation criteria and their

implementation. Those criteria included element separation based on a geometrical distance of the tool tip to the element, strain energy density or a critical plastic strain.

In contrast, an updated Lagrangian formulation with mesh adaptivity or automatic remeshing does not require a chip separation criterion. This has been successfully applied in simulation of continuous and segmented chip formation in machining processes [21,22,23,24,25,26,27].

The Arbitrary Lagrangian Eulerian (ALE) technique combines the best features of the pure Lagrangian analysis (in which the mesh follows the material) and Eulerian analysis (in which the mesh is fixed spatially and the material flows through the mesh). The ALE formulation has been utilized in simulating machining to avoid the frequent remeshing for chip separation [28,29,30,31,32,33].

In recent studies, Baker et al., [34] simulated adiabatic shearing and serrated chip formation when cutting with a sharp edge cutting tool using Lagrangian analysis with frequent remeshing and by employing a damage criteria. Ng and Aspinwall [38] used a dynamic explicit Lagrangian analysis and the Johnson-Cook constitutive model and shear failure criteria [42] in conjunction with removal of damaged elements to simulate serrated chip formation using a sharp cutting edge tool. Chuzhoy et al., [39,40] developed an explicit Lagrangian model with remeshing capability, utilized a similar damage criteria for adiabatic shearing and simulated serrated chip formation and deformations at microstructure-level when orthogonal cutting with a round edge tool.

Until late 1990 s, the vast majority of researchers used their own FEM code, however, the use of commercially available software packages has increased dramatically over the last fifteen years. These packages included NIKE-2D [11], DEFORM™ [23,24,25,26,27], FORGE2™ [21], ABAQUS™/Standard, [12,14,34] ABAQUS™/Explicit [33,35,36,37,38,39,40], ANSYS™ /LS-DYNA™ [41]. In many of these studies, the numerical codes developed were practical and available commercially for end users.

3. Finite element modeling of orthogonal cutting

In this study, the FEM software DEFORM-2D™, which is based on an updated Lagrangian formulation that employs implicit integration method designed for large deformation simulations, is used to simulate the cutting process. The strength of the FEM software is its ability to automatically remesh and generate a very dense grid of nodes near the tool tip so that large gradients of strain, strain-rate and temperature can be handled. In this approach, there is no need for a chip separation criterion, making it is highly effective in simulating metal cutting process. Furthermore, a high mesh density is defined around the cutting edge as moving windows allowing an excessively distorted mesh in the primary and secondary zones to be automatically remeshed without interruption. Thus, formation of the continuous chip is simulated step by step per tool advance with a minimum number of remeshing. In addition, this software has the capability to model the tool as an elastic object so that stress distributions in the tool can also be predicted. The flow diagram of the process simulations is shown in Fig. 2.

In this study, FE simulation for orthogonal cutting of low-carbon-free-cutting steel (LCFCS) with P20 carbide cutting tool is designed by modeling the workpiece as elastic-plastic and the tool as elastic bodies. Nodal velocities at the bottom of the workpiece model are set to zero as boundary conditions and the tool is moved from right to left due to the cutting speed. Work material flow stress behavior and contact friction conditions are predefined and input to the simulation model accordingly. Cutting conditions, physical and thermo-mechanical properties used for the work and tool materials are given in Table 1.

3.1. Work material flow stress properties

The flow stress or instantaneous yield strength at which work material starts to plastically deform or flow is mostly influenced by temperature, strain and strain rate factors. It is widely accepted that work material flow stress properties must be entirely captured with an empirical constitutive model for a wide range of strain, strain rate and temperature [42,43,44,46,47]. Accurate and reliable flow stress models are considered highly necessary to represent work material constitutive behavior under high-speed cutting conditions to successfully conduct FE simulations. There are various constitutive models to describe the flow stress properties of materials such as the Johnson-Cook model [42]. Shirakashi et al., [43] introduced a semi-empirical constitutive model including strain path effects for the flow stress of carbon steels. Their constitutive model reduces to Eq.1 when the strain path effects are eliminated.

$$\bar{\sigma} = A\left(\frac{\dot{\bar{\varepsilon}}}{1000}\right)^{M} \bar{\varepsilon}^{N} \tag{1a}$$

$$A = 930\, \mathrm{e}^{-0.0011\,T} + 120\, \mathrm{e}^{-0.00004(T-280)^2} + 50\, \mathrm{e}^{-0.0001(T-600)^2} \tag{1b}$$

$$M = 0.018 - 0.000038\,T \tag{1c}$$

$$N = 0.16\, e^{-0.0017\,T} + 0.09\, e^{-0.00003(T-370)^2} \tag{1d}$$

This flow stress expression is empirically determined as a function of strain, strain-rate and temperature from the split Hopkinson bar tests (SHBT), where the flow stress of LCFCS is measured over strain range 0–1, strain-rate range 10^{-3}–10^{3} 1/s and at temperatures from 20–700 °C.

This flow stress model has been effectively used in DEFORM-2D™ by way of flow stress curves, which are given in Fig. 3. The extrapolated ranges of strain,

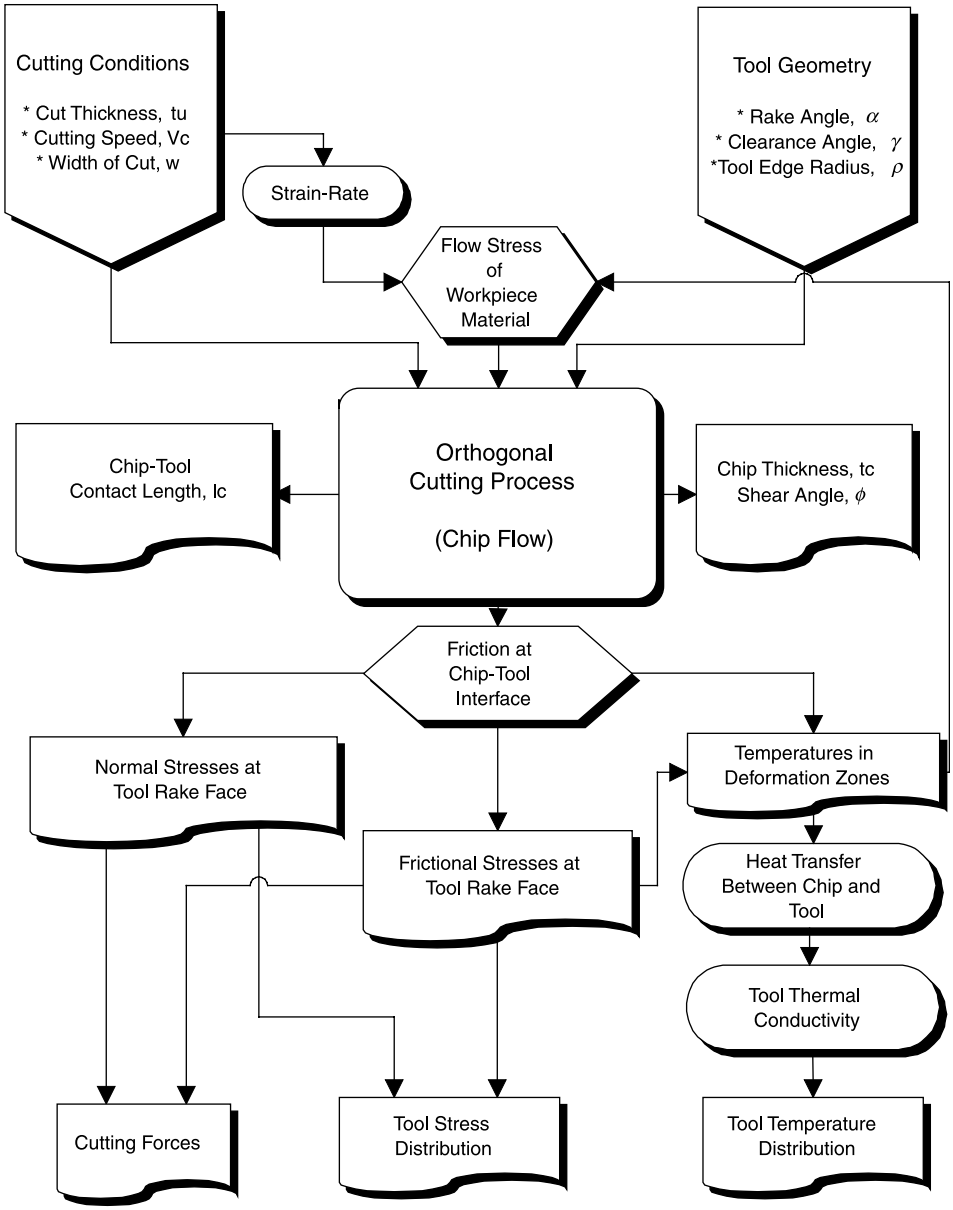

Fig. 2. Modeling of orthogonal cutting process using the FEM based process simulation technique.

strain-rate and temperature for the flow stress model are 0.1–10, 10^{-3}–10^{5} 1/sec, and 20–1200 °C, respectively.

Other material properties for work material and tool thermal properties are obtained from a metals handbook as given in Table 1.

4. Friction characteristics at the tool-chip interface

The contact regions and the friction parameters between the tool and the chip are influenced by factors such as cutting speed, feed rate, rake angle, etc., mainly because of the very high normal pressure at the surface. Friction at the tool-chip interface is complicated and difficult to estimate. It is widely accepted that the friction at the tool-chip interface can be represented with a relationship between the normal and frictional stress over the tool rake face. The best way to capture the friction characteristic at the tool-chip interface is to directly measure the normal and frictional stresses during the actual metal cutting process. There are two common approaches to measuring normal and frictional stress distributions on the tool rake face, as repeatedly reported in literature: split-tool and photo elastic method. Although, these techniques can capture approximate stress distributions, it is assumed that the split-tool technique as reported by Childs and co-workers [7,8] is capable of obtaining the true normal and frictional stress relationship at the tool-chip interface during dry orthogonal cutting. Therefore, normal and frictional stress measurements obtained from Ref. 7 and 8 are utilized in this paper.

Table 1
List of parameters used in the FE simulations [45]

Orthogonal Cutting Parameters	
Cutting speed, V_c [m/min]	50,150,250
Uncut chip thicknes, t_u [mm]	0.1
Width of cut, w [mm]	2.5
Tool rake angle, α [degree]	0
Tool clearance angle [degree]	5
Tool edge radius, ρ [mm]	0.02
Workpiece (Lcfcs) Properties	
Coefficient of thermal expansion [μm /(m°C)]	13.05 (at 20–200 °C) 13.40 (at 20–300 °C)
Density [g/cm^3]	7.85
Fraction of deformation energy transformed into heat	0.9
Heat transfer coefficient between workpiece-tool contact [W/m^2 °C]	1.0×10^5
Heat capacity [N/mm^2/°C]	3.5325 + 0.002983 T °C
Poisson's ratio	0.3
Specific heat [J/kg/°C]	450 + 0.38 T °C
Thermal conductivity [W/(m°C)]	62–0.044 T °C
Young's modulus [GPa]	200
Tool (P20 Cemented Carbide) Properties	
Coefficient of thermal expansion [μm/(m°C)]	5.8 (at 200 °C) 6.8 (at 1000 °C)
Density [g/cm^3]	12.1
Heat capacity [N/mm^2/°C]	2.7884
Poisson's Ratio	0.22
Specific heat [J/kg/°C]	230.45
Thermal conductivity [W/(m°C)]	46
Young's Modulus [GPa]	558

In the earlier analyses of machining, frictional stresses, τ_f, on the tool rake face have been considered proportional to the normal stresses, σ_n, with a coefficient of friction, μ, based on the Coulomb friction as,

$$\tau_f = \mu\sigma_n \tag{2}$$

The prevalent conditions at the tool-chip interface constrain the use of the empirical values of the coefficient of friction found from ordinary sliding test conditions.

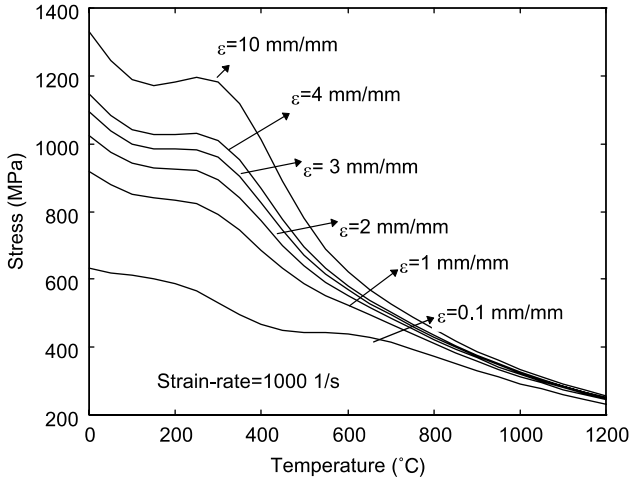

Fig. 3. Flow stress curves for the LCFCS used in this study [43].

In conventional machining at low cutting speeds, the Coulomb friction can be mostly effective at the tool flank face. However, in high speed machining, a tremendous increase in the chip velocity, the tool-chip friction contact pressure and the temperatures are encountered at the tool rake face. As a result, the increasing sliding velocity and frictional stress cause significant wear on the tool rake face. Therefore, the rate of the tool wear heavily depends on the frictional conditions at the tool-chip interface in high speed machining.

In fact, interfacial friction on the tool rake face is not continuous and is a function of normal and frictional stress distributions. According to Zorev [48], the normal stress is greatest at the tool tip and gradually decreases to zero at the point where the chip separates from the rake face as shown in Fig. 4. The frictional shearing stress distribution is more complicated. Over the portion of the tool-chip contact area near the cutting edge, sticking friction occurs, and the frictional shearing stress, τ is equal to average shear flow stress at tool-chip interface in the chip, τ_p. Over the remainder of the tool-chip contact area, sliding friction occurs, and the frictional shearing stress can be calculated using the coefficient of friction μ. Based on Zorev's analysis [48], the normal and shear stress distributions on the tool rake face can be represented in two distinct regions:

$$\tau_f(x) = \tau_p \text{ and when } \mu\sigma_n(x) \geq \tau_p \quad 0 < x \leq l_p \tag{3a}$$

$$\tau_f(x) = \mu\sigma_n(x) \text{ and when } \quad \mu\sigma_n(x) < \tau_p, \quad l_p < x \leq l_c \tag{3b}$$

Frictional conditions at the tool-chip interface in early FE models of metal cutting have been largely ignored [5,9] or assumed to be constant with a constant coefficient of friction based on Coulomb's law at the entire tool-chip interface [4,12,15,17]. Many researchers utilized Zorev's model in FE simulations of orthogonal cutting as given with Eq. 3. The location of the separation of these two regions is often estimated from examining the marks left on worn tool

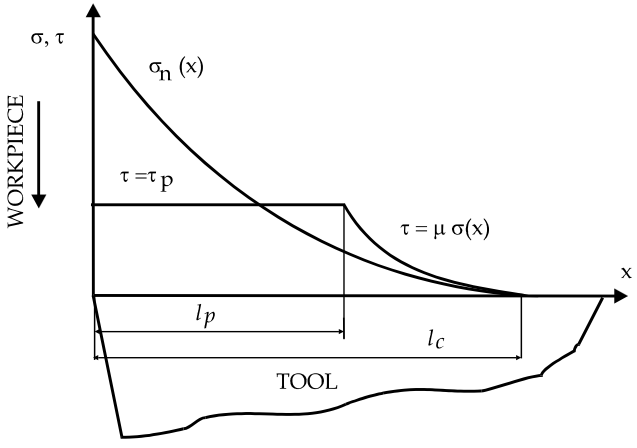

Fig. 4. Curves representing normal and frictional stress distributions on the tool rake face according to Zorev [48].

rake face, or from the measured stress distributions on the tool rake face.

The mean coefficient of friction between tool and chip in orthogonal cutting is usually calculated from the measured cutting forces as given with Eq. 4.

$$\mu = \frac{F_t + F_c \tan \alpha}{F_c - F_t \tan \alpha} \tag{4}$$

Usui and Shirakashi [4] derived an empirical stress characteristic equation as a friction model at the tool-chip interface as given with Eq.5.

$$\tau_f = k[1 - e^{-(\mu\sigma_n/k)}] \tag{5}$$

where k is the shear flow stress of the local work material and a coefficient of friction, μ, is obtained from experiments for different workpiece-tool material combinations. This expression reduces to Eq. 2 at low normal stresses and becomes equal to shear flow stress of work material, k for the high normal stress values. Dirikolu et al., [8] made a further modifications to this model by multiplying k with a friction factor m, where $0 < m < 1$, and introducing an exponent n.

$$\tau_f = mk[1 - e^{-(\mu\sigma_n/mk)^n}]^{1/n} \tag{6}$$

4.1. Modeling friction in finite element simulation of machining

In this study, the influence of implementing different friction models on predictions of FE simulation was investigated by comparing predicted process variables to experimental results. Measured cutting forces, temperatures, stress distributions on the tool rake face, tool-chip contact length and shear angle in orthogonal cutting process were obtained from the literature [7].

Initially, experimental data obtained under the cutting conditions of cutting speed, $V_c = 150$ m/min, width of cut, $w = 2.5$ mm, and uncut chip thickness, $t_u = 0.1$ mm from orthogonal end turning experiments, were used. For those conditions, the measured cutting force, $F_c = 174$ N/mm, thrust force, $F_t = 83$ N/mm, and shear angle of $\phi = 18.8°$ were reported by Childs et al., [7].

4.1.1. Constant shear friction at the entire tool-chip interface (model I)

Friction in the workpiece-tool contact is modeled using a shear friction factor, m

$$m = \frac{\tau}{k} \tag{7}$$

where k is shear flow stress of the work material at the tool-chip interface. The shear friction factor, m, must be estimated as an input into the FE simulations to represent the friction at entire the tool-chip interface. An average shear flow stress for the work material can be estimated from Eq. 5 as $k = 440$ MPa according to DeVries [49].

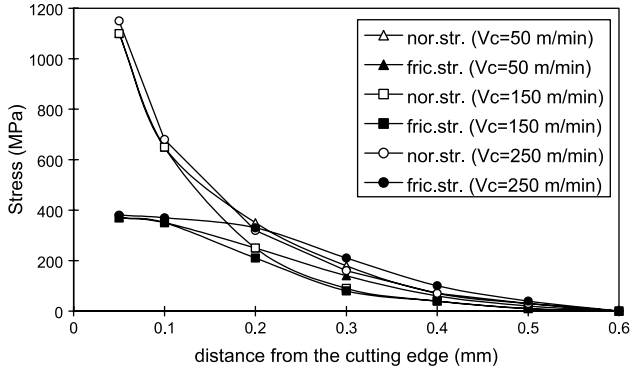

Fig. 5. Measured normal and shear stress distribution on cutting tool rake face in orthogonal cutting of LCFCS using the split-tool technique as reported by Child et al., [7].

$$k = \frac{F_c \cos\phi \sin\phi - F_t \sin^2\phi}{t_u w} \tag{8}$$

This is considered as local shear flow stress at the tool-chip interface. The measured maximum shear stress, τ, on the rake face is taken as 360 MPa from Ref [7]. Thus, a constant shear friction factor is applied over the entire tool-chip contact by considering $m = 0.818$ as estimated from Eq. 7.

By employing Zorev's stress distribution model [49] shown in Fig. 4, and using measured normal and shear stress distributions over the rake face given for various cutting speeds as shown in Fig. 5 the following friction models for tool-chip contact have been formed:

4.1.2. Constant shear friction in sticking region and Coulomb friction in sliding region (model II)

A popular approach to model friction at the tool-chip interface is the use of two distinct friction regions over the tool rake face as explained with Eq.3. This approach has been used in many FEM studies of machining in the past. The difficulty arises as how to identify the boundaries of those regions. In other words, the parameters l_p and l_c must be experimentally measured and used in the friction modeling. Therefore, the length of the sticking region, l_p, and the chip-tool contact, l_c, are estimated from the measured stress distributions (see Fig. 5) on the tool rake face and assumed constant in this model. Hence, a friction model with a combination of Coulomb and shear friction is constructed by defining two distinct friction regions in the tool-chip contact where m is applied over the sticking region ($0 < x < l_p = 0.1$ mm) while μ is applied over the sliding region ($l_p = 0.1 < x < l_c = 0.6$ mm). Both m and μ are estimated from the stress distributions as 0.818 and 1.0 respectively.

4.1.3. Variable shear friction at the entire tool-chip interface (model III)

Only a variable shear friction is considered as a function of normal surface pressure along the entire tool-chip

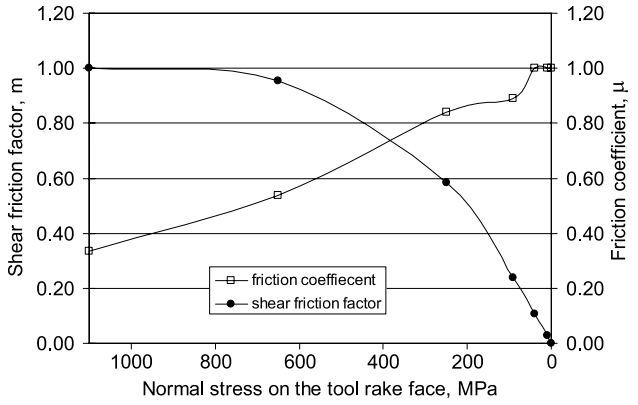

Fig. 6. Variable shear friction and variable friction coefficient as functions of normal stress on the tool rake face

contact. The shear friction factor is determined, as shown in the Fig. 6, based on the empirical friction model presented in Eq. 6. Dirikolu et al., [8] also identified the parameters, n and m in their model as 1.7 and 1.0 respectively.

$$m = \frac{\tau_p}{k}\left[1 - \exp\left\{-\left(\frac{\sigma_n}{\tau_p}\right)^{1.7}\right\}\right]^{1/1.7} \quad (9)$$

where $k = 440$ MPa and $\tau_p = 360$ MPa.

This empirical relation is entered in FE simulation software as a variable shear friction relationship.

4.1.4. Variable friction coefficient at the entire tool-chip interface (model IV)

The most direct way of presenting the friction relation at the tool-chip interface is to capture the relationship between frictional stress and normal stress along the tool rake face. Therefore, a variable friction coefficient is constructed by considering μ as a function of normal stress along the entire tool-chip interface. The variable friction coefficient defined as $\mu = \tau/\sigma_n$, is calculated as shown in Fig. 6 from the relation $\tau = f(\sigma_n)$, by using the experimental stress distribution data given in Fig. 5.

4.1.5. Variable shear friction in sticking region and variable friction coefficient in sliding region (model V)

A friction model based on the combination of variable shear friction and variable friction coefficient is developed by creating two distinct friction regions on tool rake face in the FE simulation, where m and μ were defined as functions of normal stress at the tool-chip interface (see Fig. 6) over the sticking region ($0 < \times <= l_p = 0.1$ mm) and the sliding region ($l_p = 0.1 < \times <= l_c = 0.6$ mm), respectively.

4.2. Comparison of friction models

Evaluations of these friction models are carried out under the same cutting condition and tool geometry in order to identify the most suitable friction model in predicting process variables accurately using FE simulations of machining. The orthogonal cutting parameters, work and tool material properties used in FE simulations are given in Table 1.

Table 2
Comparison of friction models with experimental results at $V_c = 150$ m/min

Experimental Results, Childs et al. [7]					
	F_c (N/mm)	F_t (N/mm)	l_c (mm)	ϕ (degree)	T_{max} (°C)
	174	83	0.6	18.8	590
Predicted Values from FE Simulations					
Friction Model	F_c (N/mm)	F_t (N/mm)	l_c (mm)	ϕ (degree)	T_{max}(°C)
I	270	108	0.38	20.9	607
II	283	126	0.38	21.3	450
III	265	101	0.34	21.1	600
IV	272	115	0.47	18.4	620
V	297	140	0.51	17.8	489

The predicted process variables (cutting force F_c, thrust force F_t, chip-tool contact lentgth l_c, shear angle ϕ and maximum temperature at tool-chip interface T_{max}) from the process simulations using five friction models (models I, II, III, IV, and V) are presented in Table 2. The measured cutting and thrust forces are believed to be within $\pm 10\%$ accuracy of the experimental conditions as reported by Childs et al., [7]. Comparison with experimental results depicts that cutting force, F_c and tool-chip contact length, l_c are not in close agreements while other predicted process variables exhibit fair agreements with experimental results. The best agreements between predictions and experiments are obtained for the shear angle and maximum temperature at the tool-chip interface. Clearly, the friction models (III, IV and V) that are developed from the experimentally measured normal and frictional stresses at the tool rake face have been identified as good.

It should be noted that predicted process variables are closest to the experimental ones when using especially variable friction models at the entire tool-chip interface (III, IV). Thus, it is suggested here that the variable friction models should be used in order to obtain more accurate results in FE simulations of machining.

5. Prediction of cutting forces, stresses and temperatures

After comparing the friction models as explained in the previous section, the process variables (chip shapes, cutting forces, stress and temperature distributions) for additional cutting speeds (50 and 250 m/min) are predicted using variable friction models. Similarly to previous modeling done for the case with a cutting speed of 150 m/min, measured normal and frictional stress distributions are used in order to determine variable shear friction factor, m, and friction coefficient, μ, as functions of normal stress at the tool-chip interface for cases with cutting speed of 50 and 250 m/min.

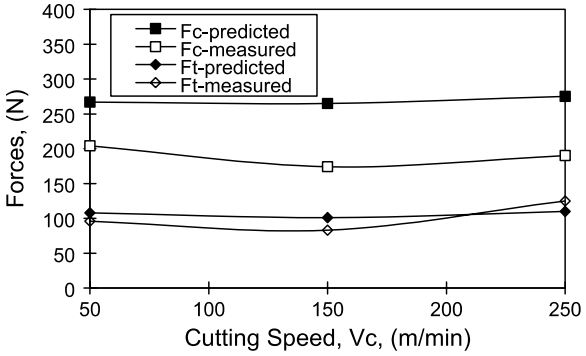

Fig. 7. Predicted and measured cutting forces using the variable shear friction model.

Predicted process variables; cutting and thrust forces, maximum tool temperature, tool-chip contact length and shear angle are compared with experimental values adopted from Childs et al., [7] as indicated in Fig. 7 and in Table 3. Predicted thrust forces match with the experimental forces where as predicted cutting forces are higher than the experimental forces. It is believed that this is due to the accuracy of the experimental data and the applicability of the flow stress model of the work material to the regimes experienced in machining. It is also evident that the temperature softening effect in the flow stress model is not sufficient enough to reflect the lower flow stress at higher temperatures generated at deformation zones. Thus further modifications to the flow stress model are essential. This can be done by utilizing orthogonal cutting as a property test and determining flow stress in conjunction with the split-hopkinson bar property test results as suggested by Childs [46], Özel and Altan [26], Guo and Liu [47], Özel and Zeren [50], and Shi and Liu [51].

Table 3
Comparison of predicted process variables using friction models III and IV with experiments

	F_c (N/mm)	F_t (N/mm)	T_{max} (°C)	l_c (mm)	ϕ (degree)
V_c=50 m/min, t_u=0.1 mm					
Measured	204	96	420	>0.60	12.6
Predicted (Model III)	267	108	399	0.38	14.4
Predicted (Model IV)	310	160	432	0.84	14.4
V_c=150 m/min, t_u=0.1 mm					
Measured	174	83	590	0.60	18.8
Predicted (Model III)	265	101	600	0.34	21.1
Predicted (Model IV)	272	115	620	0.47	18.4
V_c=250 m/min, t_u=0.1 mm					
Measured	190	125	780	>0.60	17.4
Predicted (Model III)	275	110	775	0.36	17.2
Predicted (Model IV)	268	101	830	0.36	17.3

In the second phase of the FE simulations, predicted normal and frictional stress distributions on tool rake face using the variable shear friction model at cutting speeds of 50, 150 and 250 m/min are compared with measured stress distributions obtained with split-tool experiments reported by Childs et al., [7]. These comparisons indicate that the predicted normal and frictional stresses on the tool rake face are in close agreements, as expected, with the experimentally measured values for all three cutting conditions as shown in Figs. 8.

Furthermore, FE simulations can predict all of the stress distributions in the tool, since the tool is defined as an elastic body. An example of effective stress

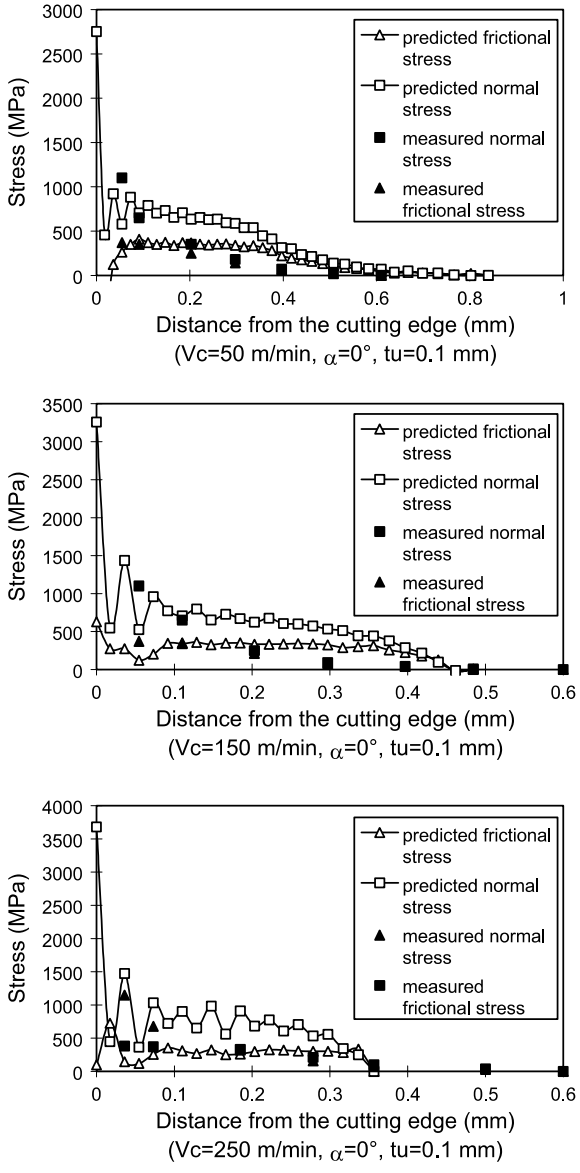

Fig. 8. Comparison of predicted stress distributions with experiments using the variable shear friction model.

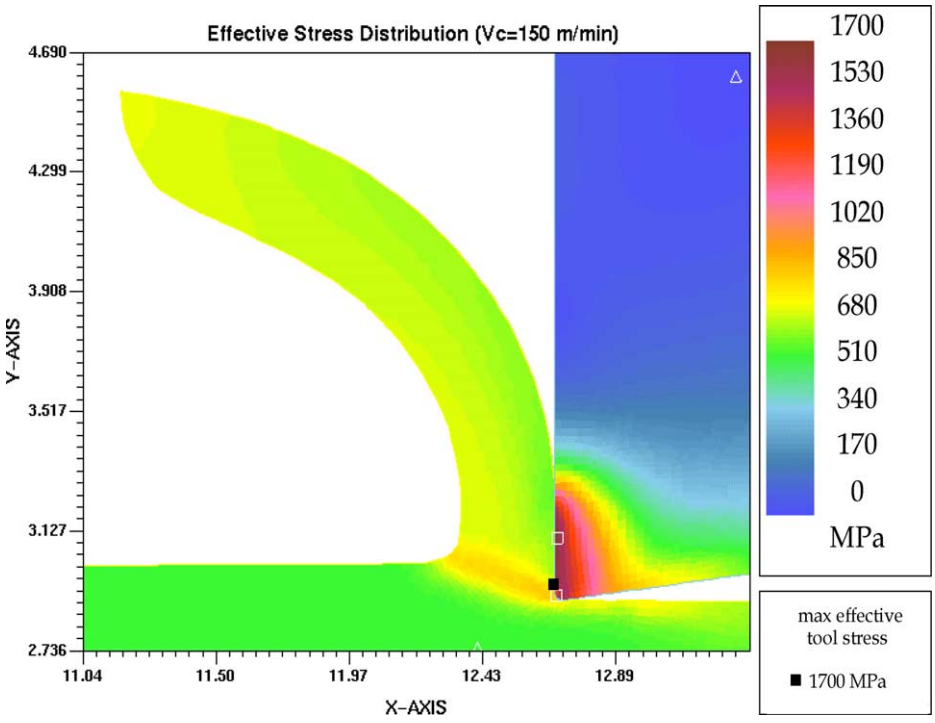

Fig. 9. Predicted effective stress distribution using the variable shear friction model at the cutting speed of 150 m/min.

distribution using variable shear friction model at the cutting speed of 150 m/min is given in Fig. 9. The temperature distribution at the same cutting condition is also given in Fig. 10. In addition, the temperature distributions that are obtained from FE simulations for all three cases (50, 150 and 250 m/min) are shown in Figs. 11, 12 and 13 respectively.

Therefore, once an applicable work material flow stress model for the deformations reached in machining regimes and a proper friction model determined for the tool-chip

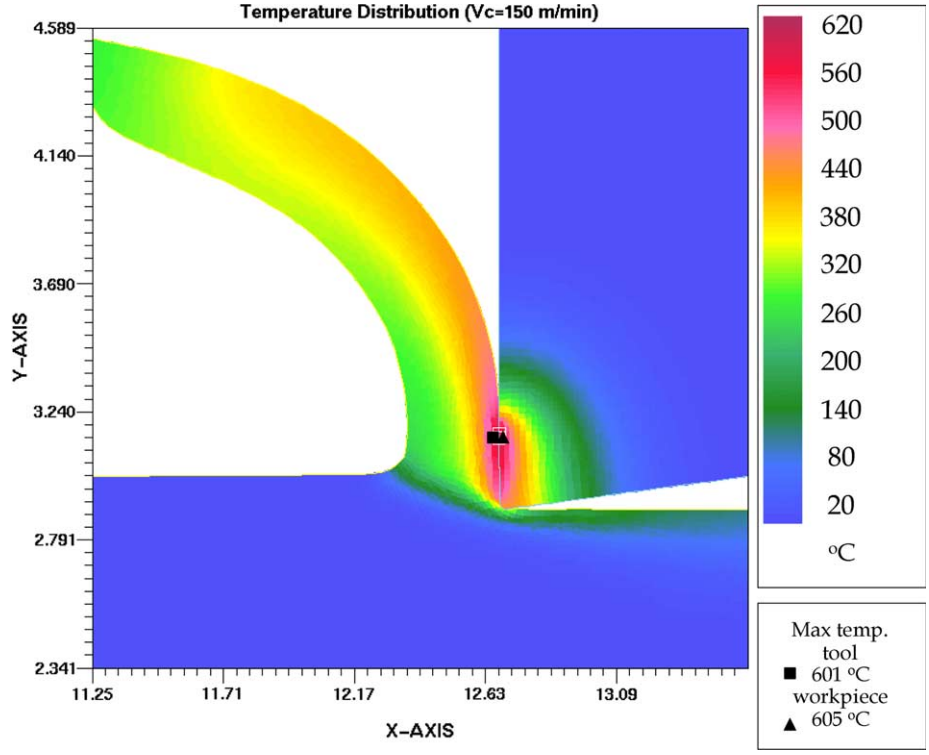

Fig. 10. Predicted temperature distribution using the variable shear friction model at the cutting speed of 150 m/min.

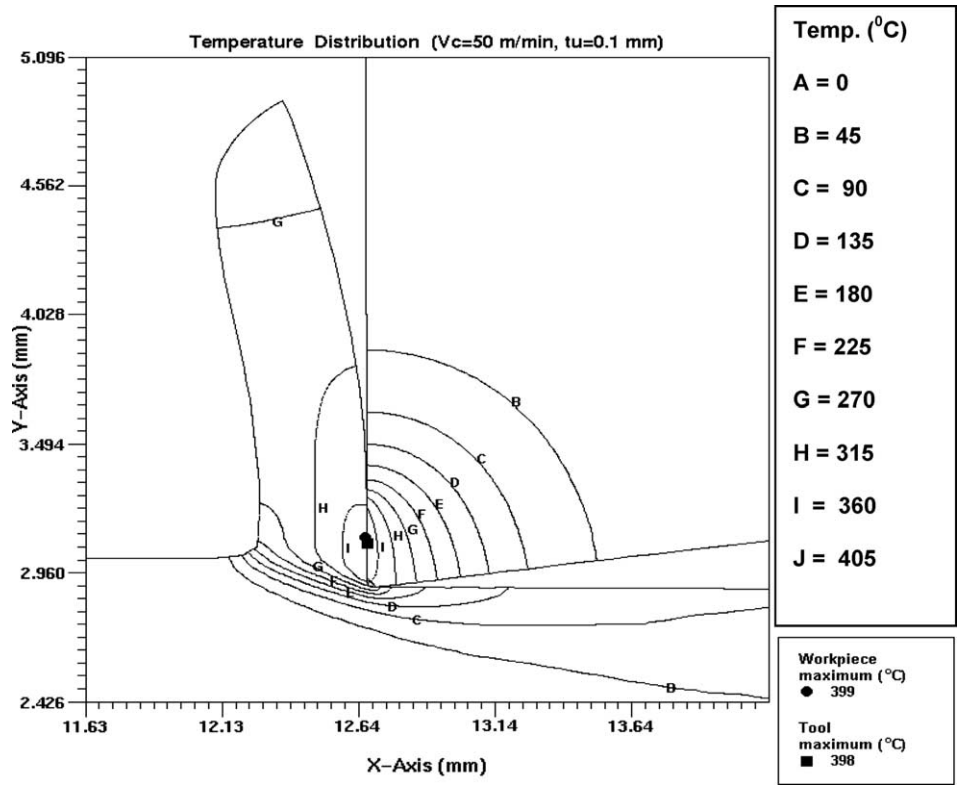

Fig. 11. Predicted temperature distribution using the variable shear friction model at the cutting speed of 50 m/min.

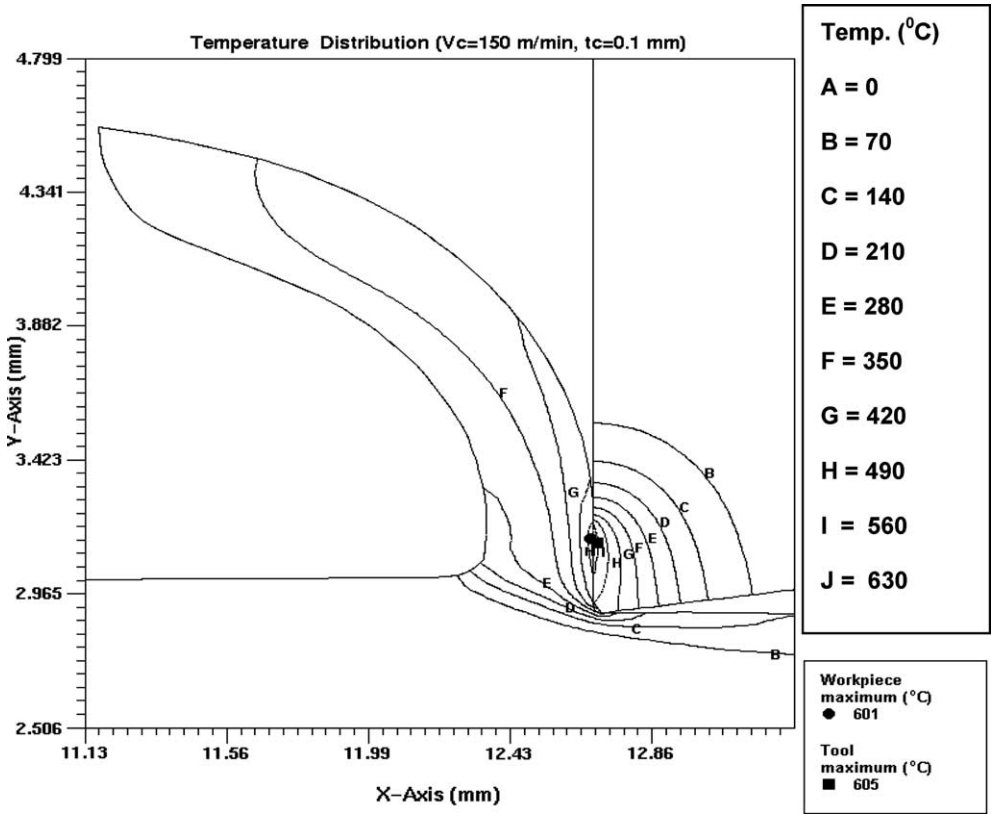

Fig. 12. Predicted temperature distribution using the variable shear friction model at the cutting speed of 150 m/min.

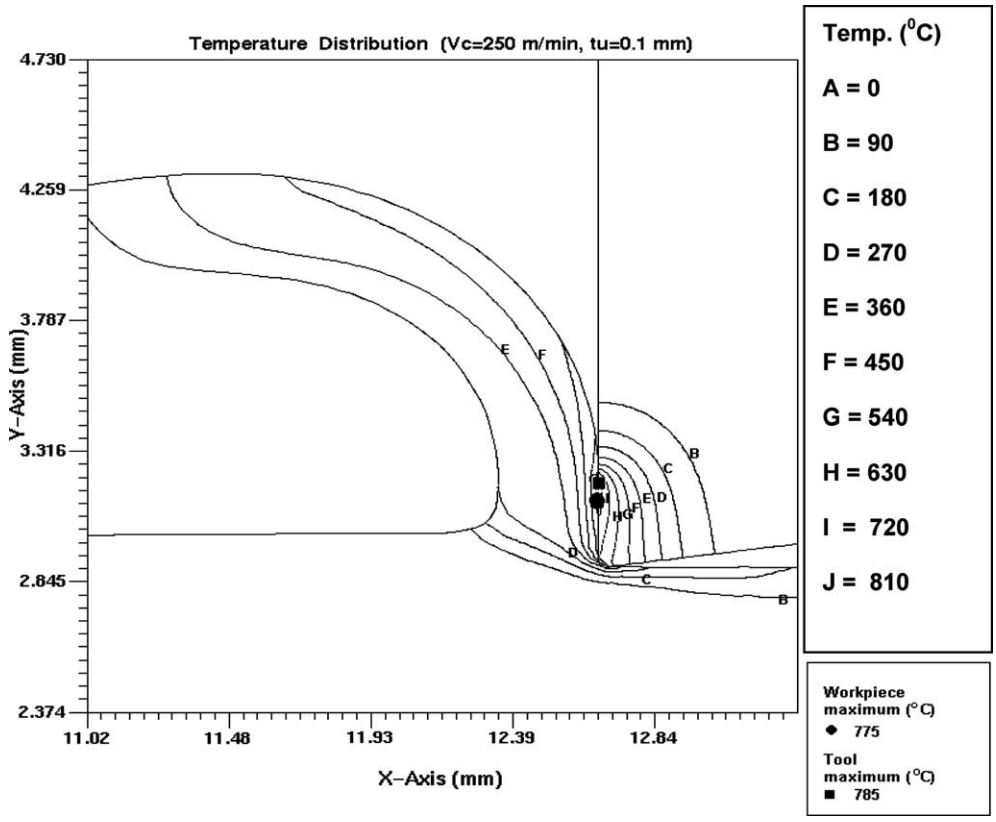

Fig. 13. Predicted temperature distribution using the variable shear friction model at the cutting speed of 250 m/min.

interface, accurate predictions of stress and temperature distributions can be obtained and furthermore simulation experiments can be designed to identify optimum tool edge geometry, cutting condition and tool material/coatings for the most desirable surface integrity, longest tool life and highest productivity.

6. Conclusions

In this study, a thermo-mechanical updated Lagrangian finite element formulation is used to simulate the continuous chip formation process in orthogonal cutting of low carbon free-machining steel. The effects of tool-chip interface friction modeling on the FE simulations are investigated by developing constant and variable shear and friction coefficient based models. The stress distributions on the tool rake face that were experimentally measured by Childs et al., [7] are utilized to implement five different friction models and the evaluation of the results for the friction models is also carried out.

FE simulations of the orthogonal cutting process at three different cutting speeds is also investigated and the predicted process variables such as shear angle, forces, maximum temperatures at the tool-chip interface and stress distributions on the tool rake face are compared with experimental results. Assessment of the friction models is performed using FE simulations as a reverse engineering tool in order to uncover the most suitable friction models. It is assumed that the measurements for the process variables, as reported by Childs et al., [7] are accurate enough to be compared with the predictions. The results of the comparisons show that the use of various tool-chip interface friction models has a significant influence in predicting chip geometry, forces, stresses on the tool and the temperatures at the tool-chip interface. The predictions are clearly found to be most accurate when utilizing friction models based on the measured normal and frictional stresses on the tool rake face and when implemented as variable friction models at the tool-chip contact in the FE simulations. Hence, this work presents some results of benchmarking friction models for the use in FE simulations of machining. Predictions presented in this work also justify that the FE simulation technique used for orthogonal cutting process is an accurate and viable analysis as long as flow stress behavior of the work material is valid in machining regimes and the friction characteristics at the tool-chip interface is modeled properly. For the future work, further justifications for the influence of friction models independently of the material models is definitely needed. It is also possible that the different combinations of friction and material models may produce better correlations with the experimental values.

Acknowledgements

The author would like to thank Professor T.H.C. Childs for providing experimental results and Dr. Y.C. Yen and Professor T. Altan for invaluable discussions.

References

[1] J. Mackerle, Finite element analysis and simulation of machining: a bibliography (1976–1996), Journal of Materials Processing Technology 86 (1999) 17–44.
[2] J. Mackerle, Finite element analysis and simulation of machining: an addendum a bibliography (1996–2002), Journal of Materials Processing Technology 43 (2003) 103–114.
[3] A.O. Tay, M.G. Stevenson, Using the finite element method to determine temperature distributions in orthogonal machining, Proceedings of Institution for Mechanical Engineers 188 (1974) 627–638.
[4] J.S. Strenkowski, J.T. Carroll, Finite element models of orthogonal cutting with application to single point diamond turning, International Journal of Mechanical Science 30 (1986) 899–920.
[5] J.S. Strenkowski, K.J. Moon, Finite element prediction of chip geometry and tool/workpiece temperature distributions in orthogonal metal cutting, ASME Journal of Engineering for Industry 112 (1990) 313–318.
[6] T.H.C. Childs, K. Maekawa, Computer-aided simulation and experimental studies of chip flow and tool wear in the turning of low alloy steels by cemented carbide tools, Wear 139 (1990) 235–250.
[7] T.H.C. Childs, M.H. Dirikolu, M.D.S. Sammons, K. Maekawa, T. Kitagawa, "Experiments on and Finite Element Modeling of turning free-cutting steels at cutting speeds up to 250 m/min", Proceedings of 1st French and German Conference on High Speed Machining, (1997) 325–331.
[8] M.H. Dirikolu, T.H.C. Childs, K. Maekawa, Finite element simulation of chip flow in metal machining, International Journal of Mechanical Sciences 43 (2001) 2699–2713.
[9] B.E. Klamecki, Incipient chip formpation in metal cutting-a three dimension finite element analysis", Ph.D. Dissertation, University of Illinois, Urbana-Champaign, 1973.
[10] E. Usui, T. Shirakashi, Mechanics of machining -from descriptive to predictive theory. In on the art of cutting metals-75 years later, vol. 7, ASME Publication PED, New York, 1982. pp. 13–35.
[11] J.S. Strenkowski, J.T. Carroll, A finite element model of orthogonal metal cutting, ASME Journal of Engineering for Industry 107 (1985) 346–354.
[12] K. Komvopoulos, S.A. Erpenbeck, Finite element modeling of orthogonal metal cutting, ASME Journal of Engineering for Industry 113 (1991) 253–267.
[13] K. Ueda, K. Manabe, Rigid-plastic FEM analysis of three-dimensional deformations field in the chip formation process, Annals of the CIRP 42 (1993) 35–38.
[14] B. Zhang, A. Bagchi, Finite element formation of chip formation and comparison with machining experiment, ASME Journal of Engineering for Industry 116 (1994) 289–297.
[15] A.J. Shih, S. Chandrasekar, H.T. Yang, Finite element simulation of metal cutting process with strain-rate and temperatures effects, Fundamental Issues in Machining, ASME, PED 43 (1990) 11–24.
[16] A.J. Shih, Finite element simulation of orthogonal metal cutting, ASME Journal of Engineering for Industry 117 (1995) 84–93.
[17] Z.C. Lin, S.Y. Lin, A couple finite element model of thermo-elastic-plastic large deformation for orthogonal cutting, ASME Journal of Engineering for Industry 114 (1992) 218–226.
[18] H. Sasahara, T. Obikawa, T. Shirakashi, FEM analysis on three dimensional cutting, International Journal of Japanese Society for Precision Engineering, 8, No. 28 (2) (1994) 473–478.
[19] H. Sasahara, T. Obikawa, T. Shirakashi, The prediction of effects of cutting condition on mechanical characteristics in machined layer Advancement of Intelligent Production, Japanese Society for Precision Engineering, Elsevier, Amsterdam, 1994. pp. 473–478.
[20] J.T. Black, J.M. Huang, An evaluation of chip separation criteria for the FEM simulation of machining, Journal of Manufacturing Science and Engineering 118 (1996) 545–553.
[21] G.S. Sekhon, J.L. Chenot, Some simulation experiments in orthogonal cutting, Numerical Methods in Industrial Forming Processes (1992) 901–906.
[22] T.D. Marusich, M. Ortiz, Modeling and simulation of high-speed machining, International Journal for Numerical Methods in Engineering 38 (1995) 3675–3694.
[23] E. Ceretti, P. Fallböhmer, W.T. Wu, T. Altan, Application of 2D FEM to chip formation in orthogonal cutting, Journal of Materials Processing Technology 59 (1996) 169–181.
[24] E. Ceretti, M. Lucchi, T. Altan, FEM simulation orthogonal cutting: serrated chip formation, Journal of Materials Processing Technology 95 (1999) 17–26.
[25] T. Özel, T. Altan, Process simulation using finite element method-prediction of cutting forces, tool stresses and temperatures in high-speed flat end milling process, International Journal of Machine Tools and Manufacture 40 (5) (2000) 713–738.
[26] T. Özel, T. Altan, Determination of workpiece flow stress and friction at the chip-tool contact for high-speed cutting, International Journal of Machine Tools and Manufacture 40 (1) (2000) 133–152.
[27] F. Klocke, H.-W. Raedt, S. Hoppe, 2D-FEM simulation of the orthogonal high speed cutting process, Machining Science and Technology 5 (3) (2001) 323–340.
[28] R. Rakotomalala, P. Joyot, M. Touratier, Arbitrary Lagrangian-Eulerian thermomechanical finite element model of material cutting, Communications in Numerical Methods in Engineering 9 (1993) 975–987.
[29] O. Pantale, R. Rakotomalala, M. Touratier, N. Hakem, A three-dimensional numerical model of orthogonal and oblique metal cutting processes, Proceeding of Engineering Systems Design and Analysis, ASME 3 (1996) 199–206.
[30] L. Olovsson, L. Nilsson, K. Simonsson, An Ale formulation for the solution of two-dimensional metal cutting problems, Computers and Structures 72 (1999) 497–507.
[31] M.R. Movahhedy, M.S. Gadala, Y. Altintas, "FE Modeling of Chip Formation in Orthogonal Metal Cutting Process: An ALE Approach", Machining Science and Technology 4 (2000) 15–47.
[32] M.R. Movahhedy, Y. Altintas, M.S. Gadala, Numerical analysis of metal cutting with chamfered and blunt tools, Journal of Manufacturing Science and Engineering 124 (2002) 178–188.
[33] A.H. Adibi-Sedeh, V. Madhavan, Understanding of finite element analysis results under the framework of Oxley's machining model 6th CIRP International Workshop on Modeling of Machining Operations, McMaster University, Hamilton, Canada, 2003.
[34] M. Baker, J. Rosler, C. Siemers, A finite element model of high speed metal cutting with adiabatic shearing, Computers and Structures 80 (2002) 495–513.
[35] C.R. Liu, Y.B. Guo, "Finite element analysis of the effect of sequential cuts and tool-chip friction on residual stresses in a machined layer", International Journal of Mechanical Sciences 42 (2000) 1069–1086.
[36] X. Yang, C.R. Liu, A new stress-based model of friction behavior in machining and its significant impact on residual stresses computed by finite element method, International Journal of Mechanical Sciences 44 (2002) 703–723.

[37] Y.B. Guo, C.R. Liu, 3D FEA modeling of hard turning, Journal of Manufacturing Science and Engineering 124 (2002) 189–199.
[38] E. Ng, D.K. Aspinwall, Modeling of hard part machining, Journal of Materials Processing Technology 124 (2002) 1–8.
[39] L. Chuzhoy, R.E. DeVor, S.G. Kapoor, D.J. Bammann, Microstructure-level modeling of ductile iron machining, ASME Journal of Manufacturing Science and Engineering 124 (2002) 162–169.
[40] L. Chuzhoy, R.E. DeVor, S.G. Kapoor, Machining simulation of ductile iron and its constituents. Part 2: numerical simulation and experimental validation of machining, ASME Journal of Manufacturing Science and Engineering 125 (2003) 192–201.
[41] M.R. Lovell, S. Bhattacharya, R. Zeng, Modeling orthogonal machining process for variable tool-chip interfacial friction using explicit dynamic finite element methods, Proceedings of the CIRP International Workshop on Modeling of Machining Operations (1998) 265–276.
[42] G.R., Johnson, W.H., Cook, A constitutive model and data for metals subjected to large strains, high strain rates and high temperatures, Proceedings of the 7th International Symposium on Ballistics, The Hague, The Netherlands, 1983, 541–547.
[43] T. Shirakashi, K. Maekawa, E. Usui, Flow stress of low carbon steel at high temperature and strain rate (Parts I–II), Bulletin of the Japan Society of Precision Engineering 17 (1983) 161–172.
[44] K. Maekawa, T. Kitagawa, T.H.C. Childs, Effects of flow stress and friction characteristics on the machinability of free cutting steels, Second International Conference on the Behavior of Materials in Machining (1991) 132–145.
[45] ASM Metals Handbook, vol.1, Metals Park, Oh.: ASM International, 1998.
[46] T.H.C. Childs, Material property needs in modeling metal machining, Proceedings of the CIRP International Workshop on Modeling of Machining Operations, Atlanta, GA (1998) 193–202.
[47] Y.B. Guo, C.R. Liu, Mechanical properties of hardened AISI 52100 steel in hard machining processes, ASME Journal of Manufacturing Science and Engineering 124 (2002) 1–9.
[48] N.N. Zorev, Inter-relationship between shear processes occurring along tool face and shear plane in metal cutting International Research in Production Engineering, ASME, New York, 1963. pp. 42–49.
[49] W.R. DeVries, Analysis of Material Removal Processes, Springer-Verlag Publications, New York, 1992.
[50] T. Özel, E. Zeren, Determination of work material flow stress and friction properties for FEA of machining using orthogonal cutting tests, Journal of Materials Processing Technology 153–154C (2004) 1019–1025.
[51] J. Shi, C.R. Liu, The influence of material models on finite element simulation of machining, ASME Journal of Manufacturing Science and Engineering 126 (2004) 849–857.